EPTT-2024-0016

# A new CFD code for simulation of the neutral atmospheric boundary layer using the RANS methodology

**Anna Caroline Felix Santos de Jesus**
**Livia S. Freire**
Instituto de Ciências Matemáticas e de Computação (ICMC) - University of São Paulo (USP)
carolinefelix@usp.br, liviafreire@usp.br

**Nelson Luis Dias**
**Willian Carlos Lesinhovski**
Federal University of Paraná (UFPR)
nldias@ufpr.br, willian.carlos@ufpr.br

***Abstract.***
*Many simulations involving the atmospheric boundary layer (ABL) are often solved using the Reynolds-averaged Navier-Stokes (RANS) methodology. It is common to find simulations in the literature that use commercial codes, which need careful modifications and simplifications to address accurately the physics of the specific problem. Developing a specific code for the neutral atmospheric boundary layer can provide advantages in terms of accuracy. In this study, we present results obtained using a code being developed specifically to model the atmosphere. The code implements the limited-length-scale (LLS) $k-\varepsilon$ turbulence model for closure of Reynolds-averaged Navier-Stokes equations. The validity of code near the wall is demonstrated by replicating the expected behavior of two variables (mean velocity $u$ and the turbulence kinectic energy $k$), using Direct Numerical Simulation (DNS) solution of the classic periodic turbulent half-channel problem as a reference. For the ABL problem, the implementation was evaluated using the Leipzig wind profile benchmark, and the obtained profiles were satisfactory.*

***Keywords:*** *atmospheric boundary layer (ABL), Reynolds-averaged Navier-Stokes (RANS), $k-\varepsilon$ turbulence model, neutral, Direct Numerical Simulation (DNS).*

## 1. Introduction

Current commercial codes for simulation of turbulent flows using the RANS (Reynolds-Averaged Navier-Stokes) methodology can be easily adapted to simulate the atmospheric boundary layer (ABL) as a rough channel flow. However, their generalized models may impose some restrictions or need specific modifications, in particular in the wall treatment and in the turbulence representation, in order to appropriately represent some particular features of the ABL (Hargreaves and Wright, 2007; Blocken *et al.*, 2007). In this sense, it is important to develop a numerical tool specific for addressing the atmospheric boundary layer problem in its three-dimensional form. This tool would be valuable for handling variations in topography, different heat exchanges with the surface, scalar transport, and other relevant processes that occur in this region of the atmosphere. This work presents the initial results of a code that is being developed specifically for the ABL using the RANS methodology.

In section 2, we present the equations that describe the behavior of the neutral ABL for flat terrain and horizontally homogeneous flow with the Coriolis effect. Section 3 briefly presents the strategies from a numerical point of view and computational domain. Section 4 discusses the problem from a physical point of view, including the wall model and the introduction of the turbulent channel problem. Finally, section 5 presents comparisons with DNS data and the Leipzig benchmark results.

## 2. Mathematical equations

The RANS methodology was chosen due to its lower computational cost compared to other approaches such as the LES (Large Eddy Simulation) methodology, as it only simulates flow statistics. The incompressible three-dimensional RANS equations, together with the transport equations for the limited-length-scale (LLS) $k-\varepsilon$ model are (Apsley and Castro, 1997; Sogachev *et al.*, 2012; Koblitz, 2013; van der Laan *et al.*, 2015; Zhou and Ishihara, 2023; Baungaard *et al.*, 2024):

$$\frac{\partial U_i}{\partial x_i} = 0, \tag{1}$$

$$\frac{\partial U_i}{\partial t} + \frac{\partial (U_i U_j)}{\partial x_j} - \frac{\partial}{\partial x_j}\left[(\nu + \nu_t)\left(\frac{\partial U_i}{\partial x_j} + \frac{\partial U_j}{\partial x_i}\right)\right] + \frac{\partial \tilde{p}}{\partial x_i} = F_i, \tag{2}$$

$$\frac{\partial k}{\partial t} + \frac{\partial (k U_j)}{\partial x_j} - \frac{\partial}{\partial x_j}\left[\left(\nu + \frac{\nu_t}{\sigma_k}\right)\frac{\partial k}{\partial x_j}\right] = P_k - \varepsilon, \tag{3}$$

$$\frac{\partial \varepsilon}{\partial t} + \frac{\partial (\varepsilon U_j)}{\partial x_j} - \frac{\partial}{\partial x_j}\left[\left(\nu + \frac{\nu_t}{\sigma_\varepsilon}\right)\frac{\partial \varepsilon}{\partial x_j}\right] = C^*_{1\varepsilon}\frac{\varepsilon}{k}P_k - C_{2\varepsilon}\frac{\varepsilon^2}{k} + D, \tag{4}$$

$$C^*_{1\varepsilon} = C_{1\varepsilon} + (C_{2\varepsilon} - C_{1\varepsilon})\frac{l}{l_e}, \tag{5}$$

$$D = C_\mu\left[\left(\frac{1}{\sigma_k} - \frac{1}{\sigma_\varepsilon}\right)k\frac{\partial^2 k}{\partial x_i^2} - \left(\frac{1}{\sigma_k} + \frac{1}{\sigma_\varepsilon}\right)\frac{k}{\varepsilon}\frac{\partial \varepsilon}{\partial x_i}\frac{\partial k}{\partial x_i} + \frac{2}{\sigma_k}\frac{\partial k}{\partial x_i}\frac{\partial k}{\partial x_i}\right]. \tag{6}$$

In the system of equations above, $x_i (x_1 = x, x_2 = y, x_3 = z)$ are the longitudinal, lateral, and vertical directions, the unknowns are the velocity vector $U_i = (U, V, W)$, the modified pressure $\tilde{p}$, the turbulence kinetic energy (TKE) $k$ and its dissipation rate, $\varepsilon$. The parameters $\nu$ represent kinematic viscosity and $F_i$ a force that is defined for each type of problem. For example, in the case of the turbulent channel problem, $F_i$ can be a constant value in any direction, representing the mean pressure gradient that drives the flow. On the other hand, in the ABL problem, it can represent the Coriolis term, which captures the effects of the Earth's rotation on velocity profiles and is expressed as:

$$F_i = f_c \epsilon_{ij3}(G_j - U_j), \tag{7}$$

where $G_j$ the geostrophic wind component, $f_c$ is the Coriolis parameter and $\epsilon_{ij3}$ is the Levi-Civita tensor.

Finally, $P_k$ is the production of turbulence kinetic energy, which is expressed as

$$P_k = \nu_t\left(\frac{\partial U_i}{\partial x_j} + \frac{\partial U_j}{\partial x_i}\right)\frac{\partial U_i}{\partial x_j}, \tag{8}$$

where,

$$\nu_t = C_\mu^{1/4} k^{1/2} l, \tag{9}$$

is the eddy viscosity in terms of the mixing length $l$, where

$$l = C_\mu^{3/4}\frac{k^{3/2}}{\varepsilon}. \tag{10}$$

The constants $\sigma_k$ and $\sigma_\varepsilon$, $C_{1\varepsilon}$, $C_{2\varepsilon}$, $C_\mu$ are empirical parameters of the model, which can be adjusted based on the specific problem being addressed. Usually, the values for $k-\varepsilon$ models are 1.0, 1.3, 1.44, 1.92 and 0.09 (Jones and Launder, 1972). As our goal is to more accurately describe the physics of the ABL, these coefficients have been adjusted with the most commonly used parameters in the literature for this formulation. For the especial parameter $l_e$ introduced by Apsley and Castro (1997), it is suggested to use (Blackadar, 1962)

$$l_e = 0.00027\frac{G}{f_c}, \quad G = \sqrt{G_1^2 + G_2^2}. \tag{11}$$

## 3. Near-wall treatment and Boundary Conditions

When solving Eqs. (1) – (10) without considering the effects of heat flow in the wall, the neutral ABL can be viewed, from a physical perspective, as equivalent to solving the classical rotating turbulent channel flow problem, because it satisfies the logarithmic law velocity profile at a small distance from the wall. This approach enables a comparison of the present simulation results with the statistics of a DNS simulation for a high Reynolds number.

The velocity profile for the turbulent channel case is expected to have a linear shape in a very narrow region near the wall. Capturing the velocity gradient of this linear profile presents a computational challenge. This task would necessitate a highly refined mesh close to the wall, leading to an increase in the number of cells and, consequently, an increase in the unknowns of the problem. It could also result in a set of poor-quality (distorted) cells that may lead to instability in the numerical method used. In the ABL simulation, we do not focus on observing the behavior of the profile in the first few millimeters above the ground; therefore, a wall model is used.

The wall model involves replacing a set of smaller volumes near the wall with a larger volume to ensure an accurate estimation of logarithmic profile for the wind speed $\mathbb{V}$ near the wall. In the neutral ABL flow, the profile can be described as (Richards and Hoxey, 1993; P. A. Durbin, 2010),

$$\mathbb{V}(z) = \frac{u_*}{\kappa} \ln\left(\frac{z}{z_0}\right), \tag{12}$$

where $\mathbb{V} = \sqrt{U^2 + V^2}$, $u_*$ is the friction velocity at the surface, $\kappa = 0.4$ is the von Kármán's constant and $z_0$ is the surface roughness length. This is also true for the turbulent channel problem, expressing $z_0$ correctly in terms of the viscous sublayer.

Although the numerical method being used does not capture precisely the velocity gradient near the wall, it is important to calculate accurately the wall shear stress, as it contributes significantly to the viscous term. The wall shear stress for the velocity is implemented as

$$\tau_{wall} = \frac{\rho\kappa C_\mu^{1/4} k_c^{1/2} \mathbb{V}(z_c)}{\ln(z_c/z_0)}, \tag{13}$$

where $z_c$ represents the height of the control volume center adjacent to the wall.

The velocity field on the ground has a no-slip boundary condition. In this work, the wall model follows the approach present in the literature by introducing a new variable, $\nu_w$, in the momentum equation to correct the shear stress $\tau_w$ in the volumes adjacent to the wall (Bredberg, 2000; H. Versteeg, 2007),

$$\nu_w = \frac{\rho\kappa C_\mu^{1/4} k_c^{1/2} z_c}{\ln(z_c/z_0)}, \tag{14}$$

where $k_c$ denotes the calculated turbulence kinetic energy at the control volume center. A specific value for $\varepsilon$ and $P_k$ must be set for cells adjacent to the wall. We implemented for $\varepsilon$ (Koblitz, 2013),

$$\varepsilon_c = \frac{C_\mu^{1/2} k_c \mathbb{V}(z_c)}{2z_c} \frac{\ln(2z_c/z_0)}{\ln(z_c/z_0)} \tag{15}$$

and as suggested by Hargreaves and Wright (2007) and Koblitz (2013), for neutral ABL follow,

$$\int_{z_0}^{2z_c} P_k dz = \frac{\tau_{\text{wall}}^2}{\rho\kappa C_\mu^{1/4} k_c^{1/2} 2z_c} \ln\left(\frac{2z_c}{z_0}\right). \tag{16}$$

On the other hand, for TKE, the boundary condition is a normal gradient equal to zero at the wall to correctly respect the balance of the equations. Other boundary conditions include periodicity in the $x$ and $y$ directions and zero normal gradients at the top of the domain for all unknowns, as organized in the Tab. 1.

## 4. Numerical Method

The numerical method used is the finite volume method. A geometric progression stretch is developed only vertically. The momentum equation is solved using the projection method. Temporal terms are discretized using the Forward Euler method, advection terms are discretized using the QUICK (Quadratic Upstream Interpolation for Convective Kinematics) method, and the viscous terms are discretized with a second-order scheme. The two simulations described in the next section ran until a steady-state condition was reached. Minimum values for the turbulence kinetic energy and dissipation are introduced to avoid convergence issues. More details can be found in Koblitz (2013); van der Laan *et al.* (2015).

Table 1. Boundary conditions used in 3D simulations of Channel Flow and ABL flow.

| | Bottom | Top |
|---|---|---|
| Velocity | $U_i = 0$ and wall function (Eq. 13) | $\frac{\partial U}{\partial z} = \frac{\partial V}{\partial z} = 0, W = 0$ |
| Pressure | $\frac{\partial \tilde{p}}{\partial z} = 0$ | $\frac{\partial \tilde{p}}{\partial z} = 0$ |
| TKE | $\frac{\partial k}{\partial z} = 0$ | $\frac{\partial k}{\partial z} = 0$ |
| Dissipation rate | wall function (Eq. 16) | $\frac{\partial \varepsilon}{\partial z} = 0$ |

In this study, two verification simulations were performed. The first was performed in the channel flow case to validate the implementation of the wall function and the calculation of the shear stress. The velocity and TKE profiles for $Re_\tau = 5200$, obtained from DNS data, were used as a reference (Lee and Moser, 2015). The second simulation was based on the Leipzig benchmark (Lettau, 1950), considering a realistic domain. The computational domains are three-dimensional ($\Omega = [0\ L_x] \times [0\ L_y] \times [0\ L_z]$), and are shown in Fig. 1. The values for the coefficients used in the closure model are listed in Tab. 2.

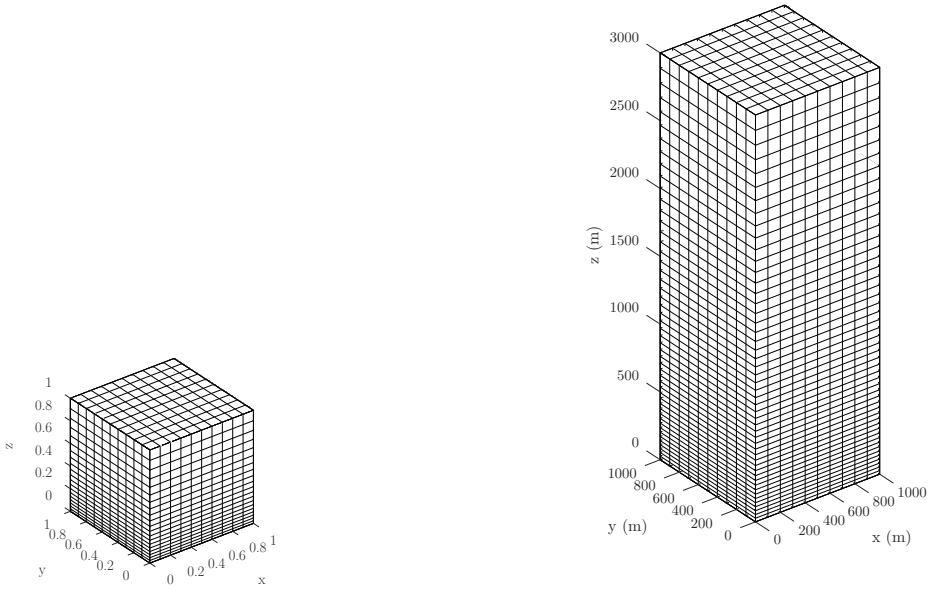


Figure 1. Representation of the computational domain for Channel flow and ABL flow simulation, respectively.

Table 2. Model constants.

| Case | $C_\mu$ | $\kappa$ | $C^*_{1\varepsilon}$ | $C_{1\varepsilon}$ | $C_{2\varepsilon}$ | $\sigma_k$ | $\sigma_\varepsilon$ |
|---|---|---|---|---|---|---|---|
| Channel Flow (Jones and Launder, 1972) | 0.09 | 0.4 | $C_{1\varepsilon}$ | 1.42 | 1.92 | 1.0 | 1.3 |
| ABL - Leipzig (van der Laan *et al.*, 2015) | 0.03 | 0.4 | Eq. 5 | 1.21 | 1.92 | 1.0 | 1.3 |

## 5. Results

The first test case corresponds to the smooth channel flow with $Re_\tau \approx 5200$. It is solved in a cubic unitary domain, and the roughness length scale necessary to reproduce a wall-modeled problem with the same Reynolds number is

$$z_0 = \frac{L_z}{Re_\tau e^{\kappa B}}. \tag{17}$$

Here, $L_z = 1$ is the height of the half-channel and $B = 5.2$. Additional input parameters for the simulation are provided in Tab. 3.

Table 3. Input parameters: Channel flow case.

| Test case | Domain [-] | Grid Number | Vertical growth ratio | $Re_\tau$ | $\nu$ | $B$ | pressure gradient mean $F_1$ [-] | Roughness length $z_0$ [-] |
|---|---|---|---|---|---|---|---|---|
| Channel Flow | $1 \times 1 \times 1$ | $10^2 \times 20$ | 1.076 | 5200 | $1/Re_\tau$ | 5.2 | 1.0 | $2.40 \times 10^{-5}$ |

An analytical result can also be obtained to support the numerical solution. The total shear stress is composed of the sum of its viscous and turbulent components,

$$\tau(z) = \tau_{visc} + \tau_{turb} = \rho\nu\frac{\partial U}{\partial z} + \rho\nu_t\frac{\partial U}{\partial z}. \tag{18}$$

Since

$$\tau(0) = \tau_{wall}, \quad \text{and} \quad \tau(L_z) = \rho\nu_t\frac{\partial U}{\partial z} = 0, \tag{19}$$

we have that

$$\frac{\tau(z)}{\tau_{wall}} = \left(1 - \frac{z}{L_z}\right). \tag{20}$$

The velocity profile in Fig. 2(a) shows the numerical solution overlaying the DNS solution in the log region. On the other hand, the TKE profile (in Fig. 2(b)) is not well represented near the wall, as usually observed in RANS models. The fact that we are modeling rather than solving the viscous and buffer regions has a significant impact in the TKE profile. The total shear stress illustrates the contributions of the molecular and turbulent terms in Fig. 2(c), and its sum as a linear profile demonstrates the correct estimate for the balance of forces in the momentum equations.

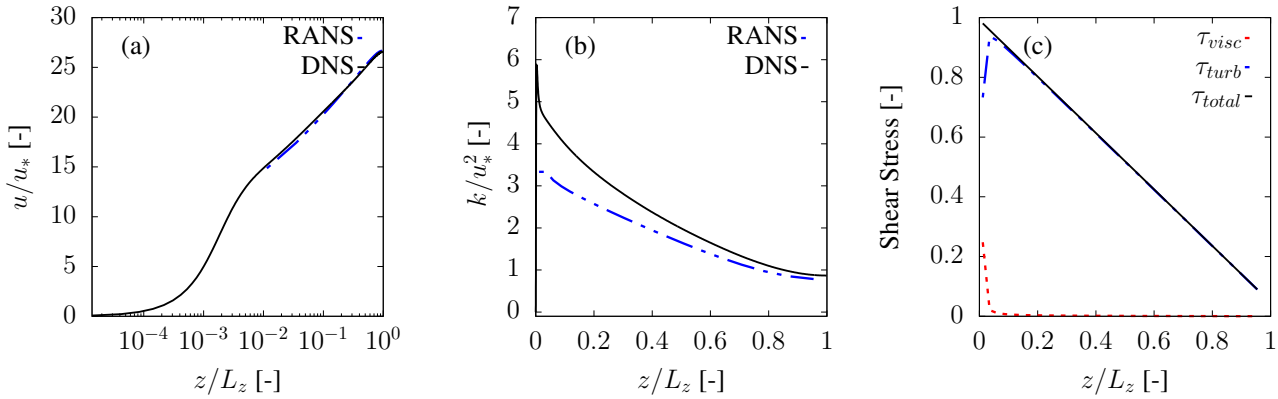


Figure 2. Numerical solution: (a) mean velocity profile, (b) TKE profile and (c) total shear stress. The reference DNS solutions are represented by the solid black lines, while the solutions obtained with the RANS simulation are represented by the blue dashed lines.

After validating the wall function with the turbulent channel problem, we disabled the constant mean pressure gradient term and enabled the Coriolis term. Thus, the second simulation is dedicated to capturing the physics of the mean velocity profile behavior in the entire ABL. We chose a domain height of 3km to allow for an appropriate development of the ABL height. The parameters for this simulation are summarized in Tab. 4.

Table 4. Input parameters: Leipzig case.

| Test case | Domain (km) | Grid Number | Vertical growth ratio | Geostrophic wind $G_1$ (ms$^{-1}$) | Coriolis parameter $f_c$ (s$^{-1}$) | Roughness length $z_0$ (m) | Maximum length scale $l_{\max}$ (m) |
|---|---|---|---|---|---|---|---|
| Leipzig | $1 \times 1 \times 3$ | $10^2 \times 50$ | 1.05 | 17.5 | $1.13 \times 10^{-1}$ | 0.3 | 41.8 |

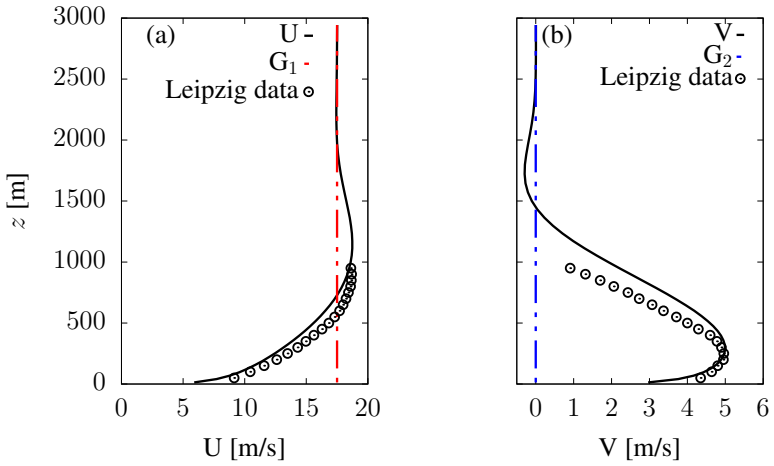


Figure 3. Mean velocity profiles for the Leipzig test case using the LLS $k-\varepsilon$ model (black continuous lines) together with the Leipzig wind profile (black points). The vertical curves (dashed lines) are the imposed geostrophic wind components.

The vertical profiles of mean velocity obtained by the LLS $k-\varepsilon$ model are shown Fig. 3. The observed profiles are close to the benchmark data. The ABL region is well represented, the ABL height develops in the range of 1-2km, and the geostrophic balance at the top of the ABL is preserved.

Other profiles that may be of interest are shown in Fig. 4. The TKE profile Fig. 4(a) decreases with height, corresponding to a turbulence decay in the upper ABL range. The dissipation of TKE profile (Fig. 4(b)) exhibits a behavior similar to that described by Richards and Hoxey (1993) when they proposed an analytical solution for the $k-\varepsilon$ model of the atmosphere. Lastly, the turbulent viscosity profile (Fig. 4(c)) shows a behavior consistent with the used formulation.

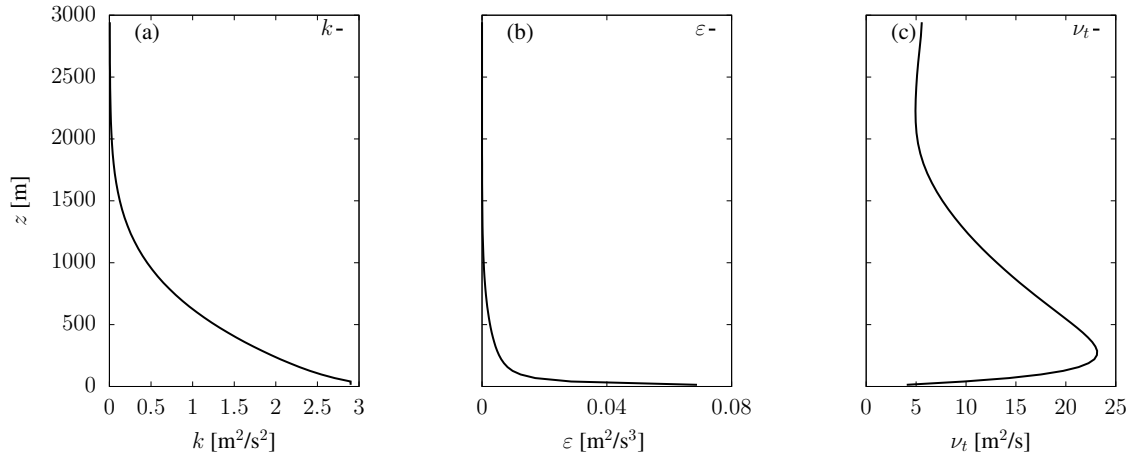


Figure 4. Results of flow statistics for the Leipzig test. (a) TKE, (b ) Dissipation rate of TKE and (c) Turbulent viscosity.

## 6. Final Considerations

In this study, we evaluated the neutral ABL flow behavior using the RANS methodology with LLS $k-\varepsilon$ equations. We compared results with data from a DNS simulation for the turbulent half-channel problem and found an expected agreement based on the wall model of the code. After using realistic parameters and incorporating the rotation effect caused by the Coriolis term, we successfully observed the expected physical behavior for the wind components profiles in the ABL. These steps were crucial for validating the code. We plan to modify the wall function to account for heat flow effects at the wall and introduce a new forcing to address the impacts of thermal stratification (buoyancy term).

## 7. ACKNOWLEDGEMENTS

This study was funded by the Coordination for the Improvement of Higher Education Personnel (CAPES /grant PROEX 88887.671252/2022-00) and the São Paulo Research Foundation (FAPESP /grant Nº. 2018/24284-1).

## 8. REFERENCES

Apsley, D.D. and Castro, I.P., 1997. "A limited-length-scale $k - \varepsilon$ model for the neutral and stably-stratified atmospheric boundary layer". *Boundary-Layer Meteorology*, Vol. 83, pp. 75–98.

Baungaard, M., van der Laan, M.P., Kelly, M. and Hodgson, E., 2024. "Simulation of a conventionally neutral boundary layer with two-equation URANS". *Journal of Physics Conference Series*, Vol. 2767, p. 052013.

Blackadar, A.K., 1962. "The vertical distribution of wind and turbulent exchange in a neutral atmosphere". *Journal of Geophysical Research*, Vol. 67, pp. 3095–3102.

Blocken, B., Stathopoulos, T. and Carmeliet, J., 2007. "CFD simulation of the atmospheric boundary layer: wall function problems". *Atmospheric Environment*, Vol. 41, pp. 238–252.

Bredberg, J., 2000. "On the wall boundary condition for turbulence models".

H. Versteeg, W.M., 2007. *An Introduction to Computational Fluid Dynamics: The Finite Volume Method (2nd Edition)*. Prentice Hall, 2nd edition.

Hargreaves, D. and Wright, N., 2007. "On the use of the $k - \varepsilon$ model in commercial CFD software to model the neutral atmospheric boundary layer". *Journal of Wind Engineering and Industrial Aerodynamics*, Vol. 95, pp. 355–369.

Jones, W. and Launder, B., 1972. "The prediction of laminarization with a two-equation model of turbulence". *International Journal of Heat and Mass Transfer*, Vol. 15, pp. 301–314.

Koblitz, T., 2013. *CFD Modeling of Non-Neutral Atmospheric Boundary Layer Conditions*. Ph.D. thesis, Denmark.

Lee, M. and Moser, R.D., 2015. "Direct numerical simulation of turbulent channel flow up to $Re_\tau \approx 5200$". *Journal of Fluid Mechanics*, Vol. 774, p. 395–415.

Lettau, H., 1950. "A re-examination of the "Leipzig wind profile" considering some relations between wind and turbulence in the frictional layer". *Tellus*, Vol. 2, No. 2, pp. 125–129.

P. A. Durbin, B.A.P.R., 2010. *Statistical Theory and Modeling for Turbulent Flows*. John Wiley & Sons.

Richards, P. and Hoxey, R., 1993. "Appropriate boundary conditions for computational wind engineering models using the $k - \varepsilon$ turbulence model". *Journal of Wind Engineering and Industrial Aerodynamics*, Vol. 46-47, pp. 145–153. ISSN 0167-6105. Proceedings of the 1st International on Computational Wind Engineering.

Sogachev, A., Kelly, M. and LeClerc, M., 2012. "Consistent two-equation closure modelling for atmospheric research: buoyancy and vegetation implementations". *Boundary-Layer Meteorology*, Vol. 145.

van der Laan, M.P., Hansen, K.S., Sorensen, N. and Réthoré, P.E., 2015. "Predicting wind farm wake interaction with RANS: an investigation of the Coriolis force". *Journal of Physics: Conference Series*, Vol. 625.

Zhou, T. and Ishihara, T., 2023. "Numerical investigation of neutral atmospheric boundary layer flows over flat terrain and three-dimensional hills considering the effects of Coriolis force". *Journal of Wind Engineering and Industrial Aerodynamics*, Vol. 240, p. 105482.

## 9. RESPONSIBILITY NOTICE

The authors Anna Caroline Felix Santos de Jesus, Livia S. Freire, Nelson Luis Dias and Willian Carlos Lesinhovski are the only ones responsible for the printed material included in this paper.